

# SlideCont: An Auto97 Driver for Bifurcation Analysis of Filippov Systems

FABIO DERCOLE

Politecnico di Milano

and

YURI A. KUZNETSOV

Utrecht University and IMPB RAS, Pushchino

---

SLIDECONT, an AUTO97 driver for sliding bifurcation analysis of discontinuous piecewise-smooth autonomous systems, known as Filippov systems, is described in detail. Sliding bifurcations are those in which some sliding on the discontinuity boundary is critically involved. The software allows for detection and continuation of codimension-1 sliding bifurcations as well as detection of some codimension-2 singularities, with special attention to planar systems ( $n = 2$ ). Some bifurcations are also supported for  $n$ -dimensional systems.

This article gives a brief introduction to Filippov systems, describes the structure of SLIDECONT and all computations supported by SLIDECONT 2.0. Several examples, which are distributed together with the source code of SLIDECONT, are presented.

Categories and Subject Descriptors: G.1.7 [Numerical Analysis]: Ordinary Differential Equations—Boundary value problems; G.1.0 [Numerical Analysis]: General—Numerical algorithms; J.2 [Physical Sciences and Engineering]; J.3 [Life and Medical Sciences]

General Terms: Algorithms

Additional Key Words and Phrases: AUTO97, numerical continuation, piecewise-smooth differential equations, Filippov systems, sliding bifurcations

---

## 1. INTRODUCTION

SLIDECONT is a suite of routines accompanying AUTO97 [Doedel and Kernévez 1986; Doedel et al. 1997], which allow one to perform bifurcation analysis of generic discontinuous piecewise smooth autonomous systems of ordinary differential equations [Filippov 1964; Filippov 1988], here called *Filippov systems*, with special attention to planar systems.

---

This work was partially supported by MIUR under project FIRB RBNE01CW3M.

Authors' addresses: F. Dercole, Department of Electronics and Information, Politecnico di Milano, Via Ponzio 34/5, 20133 Milan, Italy; email: dercole@elet.polimi.it; Yu. A. Kuznetsov, Department of Mathematics, Utrecht University, the Netherlands; and Institute of Mathematical Problems of Biology, Russian Academy of Sciences, Pushchino, Moscow Region, 142290 Russia; email: kuznetsov@math.uu.nl.

Permission to make digital or hard copies of part or all of this work for personal or classroom use is granted without fee provided that copies are not made or distributed for profit or direct commercial advantage and that copies show this notice on the first page or initial screen of a display along with the full citation. Copyrights for components of this work owned by others than ACM must be honored. Abstracting with credit is permitted. To copy otherwise, to republish, to post on servers, to redistribute to lists, or to use any component of this work in other works requires prior specific permission and/or a fee. Permissions may be requested from Publications Dept., ACM, Inc., 1515 Broadway, New York, NY 10036 USA, fax: +1 (212) 869-0481, or [permissions@acm.org](mailto:permissions@acm.org).

© 2005 ACM 0098-3500/05/0300-0095 \$5.00

Bifurcation analysis of Filippov systems is important in many applications from various fields of science and engineering. Unfortunately, a full set of sliding bifurcations in  $n$ -dimensional systems has not yet been completely catalogued. There is a growing number of interesting results on bifurcations of periodic solutions in specific 3-dimensional and in general  $n$ -dimensional Filippov systems (see, for example Feigin [1994], di Bernardo et al. [1998a, b], di Bernardo et al. [1999], di Bernardo et al. [2001], and, in particular, di Bernardo et al. [2002]). Much less is known about local bifurcations in  $n$ -dimensional systems.

The analysis of codimension-one sliding bifurcations for planar systems ( $n = 2$ ) has been completed recently [Kuznetsov et al. 2003], and appropriate *defining systems* have been proposed for numerically computing bifurcation curves with standard continuation techniques. In this article, we revise these defining systems and discuss their implementation in SLIDECONT, indicating explicitly when they are also applicable to general  $n$ -dimensional Filippov systems. Moreover, we formulate, implement, and test new defining systems for continuing periodic solutions that involve sliding on the discontinuity boundary in  $n$ -dimensional Filippov systems.

The latest version of SLIDECONT is freely available for download at:

<http://www.math.uu.nl/people/kuznet/cm>.

The compressed tar-file `slidecont.tar.gz` at this location contains the latest version of SLIDECONT. The complete User Guide to SLIDECONT [Dercole and Kuznetsov 2004], to which we refer the reader for all installation and implementation details, is found in the file `slidecont.pdf`.

This article, which is evolved from Dercole and Kuznetsov [2002], is organized as follows. In the next section we recall the definition of Filippov systems and some of their properties (for details and references, see Kuznetsov et al. [2003]). We then focus on SLIDECONT, assuming that the reader is acquainted with AUTO97. In particular, we give an overview of capabilities of SLIDECONT in Section 3 and describe its structure in Section 4. For the complete list of available defining systems and their implementation details, we refer the reader to Dercole and Kuznetsov [2004], but in Section 5 we describe two representative cases. In Section 6 we present examples of the use of SLIDECONT taken from three applications in mechanics and natural resource management. Finally, we discuss current limitations and possible extensions of SLIDECONT in Section 7.

## 2. PRELIMINARIES

We consider a generic *Filippov system*

$$\dot{x} = \begin{cases} f^{(1)}(x), & x \in S_1, \\ f^{(2)}(x), & x \in S_2, \end{cases} \quad (1)$$

where  $x \in \mathbf{R}^n (n \geq 2)$ ,

$$S_1 = \{x \in \mathbf{R}^n : H(x) < 0\}, \quad S_2 = \{x \in \mathbf{R}^n : H(x) > 0\},$$

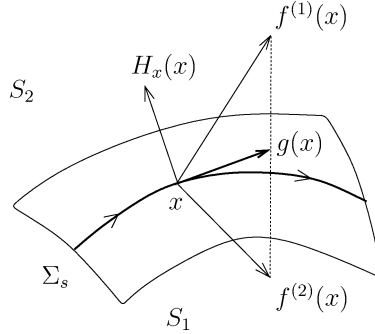


Fig. 1. Filippov construction.

$H$  is a smooth scalar function with non-vanishing gradient  $H_x(x)$  on the discontinuity boundary

$$\Sigma = \{x \in \mathbf{R}^n : H(x) = 0\},$$

and  $f^{(i)} : \mathbf{R}^n \rightarrow \mathbf{R}^n$ ,  $i = 1, 2$ , are smooth functions.

Solutions of (1) can be constructed by concatenating *standard solutions* in  $S_{1,2}$  and *sliding solutions* on  $\Sigma$  obtained with the Filippov convex method [Filippov 1964, 1988; Kuznetsov et al. 2003] described below. Let

$$\sigma(x) = \langle H_x(x), f^{(1)}(x) \rangle \langle H_x(x), f^{(2)}(x) \rangle,$$

where  $\langle \cdot, \cdot \rangle$  denotes the standard scalar product in  $\mathbf{R}^n$ . The *crossing set*  $\Sigma_c \subset \Sigma$  is defined by

$$\Sigma_c = \{x \in \Sigma : \sigma(x) > 0\}.$$

By definition, the orbit of (1) crosses  $\Sigma$  at points in  $\Sigma_c$ . The *sliding set*  $\Sigma_s$  is the complement to  $\Sigma_c$  in  $\Sigma$ :

$$\Sigma_s = \{x \in \Sigma : \sigma(x) \leq 0\}.$$

A point  $x \in \Sigma_s$  such that

$$\langle H_x(x), f^{(2)}(x) - f^{(1)}(x) \rangle = 0$$

is called a *singular sliding point*. At such points, either both vectors  $f^{(1)}(x)$  and  $f^{(2)}(x)$  are tangent to  $\Sigma$ , or one of them vanishes while the other is tangent to  $\Sigma$ , or they both vanish. The Filippov method (see Figure 1) associates the following convex combination  $g(x)$  of the two vectors  $f^{(i)}(x)$  to each nonsingular sliding point  $x \in \Sigma_s$ :

$$g(x) = \lambda f^{(1)}(x) + (1 - \lambda) f^{(2)}(x), \quad \lambda = \frac{\langle H_x(x), f^{(2)}(x) \rangle}{\langle H_x(x), f^{(2)}(x) - f^{(1)}(x) \rangle}. \quad (2)$$

Thus,

$$\dot{x} = g(x), \quad x \in \Sigma_s, \quad (3)$$

is a smooth system of differential equations in codimension-1 domains of  $\Sigma_s$ , which are composed of nonsingular sliding points. Solutions of (3) are called *sliding solutions*, while its right-hand side  $g$  is called the *Filippov vector field*.

Equilibria of (3), where the vectors  $f^{(i)}(x)$  are transversal to  $\Sigma_s$  and anti-collinear, are called *pseudo-equilibria* of (1). An equilibrium  $X$  of (3) at which one of the vectors  $f^{(i)}(X)$  vanishes, is called a *boundary equilibrium*.

The boundary of a sliding domain is composed of *tangent points*,  $T$ , where both vectors  $f^{(i)}(T)$  are nonzero but one of them is tangent to  $\Sigma$ :

$$\langle H_x(T), f^{(i)}(T) \rangle = 0,$$

boundary equilibria, and singular sliding points. Tangent points are called *visible* (*invisible*) if the orbits of  $\dot{x} = f^{(i)}(x)$  starting from them at time  $t = 0$  belong to  $S_i$  ( $S_j$ ,  $j \neq i$ ) for all sufficiently small  $|t| \neq 0$ .

Orbits of (1) can overlap when sliding. Three types of periodic orbits can occur in (1): *standard*, *crossing* (i.e., passing through both domains  $S_i$  but with no points in  $\Sigma_s$ ), and *sliding* (i.e., with at least one point in  $\Sigma_s$ ).

Two Filippov systems are called *topologically equivalent* if there is a homeomorphism  $h : \mathbf{R}^n \rightarrow \mathbf{R}^n$  mapping the discontinuity boundary of one system onto the discontinuity boundary of the other, such that orbits of one system are mapped onto the corresponding orbits of the other with time orientation preserved, and such that standard and sliding segments of any orbit are mapped onto the corresponding segments of its image.

Now, consider a Filippov system depending on parameters

$$\dot{x} = \begin{cases} f^{(1)}(x, \alpha), & x \in S_1(\alpha), \\ f^{(2)}(x, \alpha), & x \in S_2(\alpha), \end{cases} \quad (4)$$

where  $x \in \mathbf{R}^n$ ,  $\alpha \in \mathbf{R}^m$ , and  $f^{(i)}$ ,  $i = 1, 2$ , are smooth functions of  $(x, \alpha)$ , while

$$S_1(\alpha) = \{x \in \mathbf{R}^n : H(x, \alpha) < 0\}, \quad S_2(\alpha) = \{x \in \mathbf{R}^n : H(x, \alpha) > 0\},$$

for some smooth function  $H(x, \alpha)$  with  $H_x(x, \alpha) \neq 0$  for all  $(x, \alpha)$  such that  $H(x, \alpha) = 0$ . Just as for (2), one can define the parameter-dependent Filippov vector field  $g(x, \alpha)$  and a parameter-dependent version of system (3) on  $\Sigma_s(\alpha)$ . System (4) exhibits a *bifurcation* at  $\alpha = \bar{\alpha}$  if an arbitrarily small parameter perturbation produces a topologically nonequivalent system. All bifurcations of (4) are classified as *local* or *global*. A local bifurcation can be detected by looking at an arbitrarily small neighborhood of a point in the state space. All other bifurcations are called global. We focus on local and global *sliding bifurcations* of Filippov systems, in which some sliding on the discontinuity boundary  $\Sigma(\alpha)$  is critically involved.

### 3. OVERVIEW

SLIDECONT can be used to perform a partial bifurcation analysis of  $n$ -dimensional Filippov systems (4) and a much more complete bifurcation analysis of planar Filippov systems ( $n = 2$ ). Specifically, SLIDECONT is a ready-to-use collection of defining systems for continuing particular solutions of Filippov systems and their bifurcations with respect to at most two *control parameters* ( $m \leq 2$ ).

Tables I and II list the defining systems implemented in SLIDECONT, using the terminology introduced in Kuznetsov et al. [2003]. They also specify the state space dimension ( $n$ ) for which each defining system is valid and its number of control parameters ( $m$ ). Most of these defining systems were proposed

Table I. SLIDECONT Defining Systems: Algebraic Problems

Defining System	$n, m$
Discontinuity boundary $H(x, \alpha) = 0$	2, 0
Curve of tangent points of vector field $f^{(i)}$ in 3-dimensional systems $\begin{cases} H(x, \alpha) = 0, \\ \langle H_x(x, \alpha), f^{(i)}(x, \alpha) \rangle = 0. \end{cases}$	3, 0
Tangent point of vector field $f^{(i)}$ $\begin{cases} H(x, \alpha) = 0, \\ \langle H_x(x, \alpha), f^{(i)}(x, \alpha) \rangle = 0. \end{cases}$	2, 1
Standard equilibrium of vector field $f^{(i)}$ (AUTO97 defining system + boundary detection)	$n, 1$
Pseudo-equilibrium $\begin{cases} H(x, \alpha) = 0, \\ \lambda_1 f^{(1)}(x, \alpha) + \lambda_2 f^{(2)}(x, \alpha) = 0, \\ \lambda_1 + \lambda_2 - 1 = 0. \end{cases}$	$n, 1$
Boundary equilibrium of vector field $f^{(i)}$ $\begin{cases} f^{(i)}(x, \alpha) = 0, \\ H(x, \alpha) = 0. \end{cases}$	$n, 2$
Pseudo-saddle-node bifurcation (Limit point of Pseudo-equilibrium)	$n, 2$
Double tangency bifurcation of vector field $f^{(i)}$ (Limit point of Tangent point of vector field $f^{(i)}$ )	2, 2
Coinciding tangent points $\begin{cases} H(x, \alpha) = 0, \\ \langle H_x(x, \alpha), f^{(1)}(x, \alpha) \rangle = 0, \\ \langle H_x(x, \alpha), f^{(2)}(x, \alpha) \rangle = 0. \end{cases}$	2, 2

for planar Filippov systems ( $n = 2$ ) in Kuznetsov et al. [2003]. The computation of sliding solutions in the planar case reduces to the continuation of the one-dimensional discontinuity boundary  $\Sigma$ , however, so that any continuation problem reduces to continuation of the appropriate standard solutions. In contrast, in this article we also address the problem of continuing sliding solutions in general  $n$ -dimensional Filippov systems, with particular consideration of sliding periodic solutions.

As an AUTO97 driver, SLIDECONT sets up a user-selected defining system in AUTO97 format, enabling the computation to be performed by means of standard AUTO97 routines.

Among other things, AUTO97 computes curves of solutions to *algebraic problems*:

$$F(U, \mu) = 0, \quad U, F \in \mathbf{R}^{n_d}, \quad \mu \in \mathbf{R}^1, \quad (5)$$

Table II. SLIDECONT Defining Systems: Boundary-Value Problems

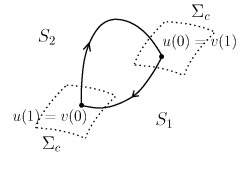
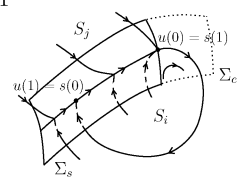
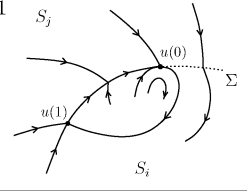
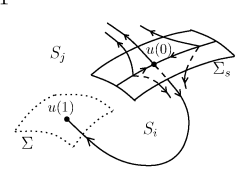
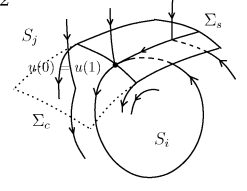
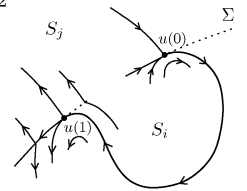
Defining System	$n, m$
Standard cycle of vector field $f^{(i)}$ (AUTO97 defining system + grazing detection)	$n, 1$
Crossing cycle $\begin{cases} \dot{u} - T_1 f^{(1)}(u, \alpha) = 0 \\ \dot{v} - T_2 f^{(2)}(v, \alpha) = 0 \\ H(u(0), \alpha) = 0 \\ H(u(1), \alpha) = 0 \\ u(1) - v(0) = 0 \\ v(1) - u(0) = 0 \end{cases}$	$n, 1$ 
Sliding cycle of vector field $f^{(i)}$ $\begin{cases} \dot{u} - T_i f^{(i)}(u, \alpha) = 0 \\ \dot{s} - T_0 g(s, \alpha) = 0 \\ H(u(0), \alpha) = 0 \\ \langle H_x(u(0), \alpha), f^{(i)}(u(0), \alpha) \rangle = 0 \\ s(0) - u(1) = 0 \\ s(1) - u(0) = 0 \end{cases}$	$n, 1$ 
Orbit of vector field $f^{(i)}$ connecting a tangent point of $f^{(i)}$ with the boundary $\Sigma$ $\begin{cases} \dot{u} - T f^{(i)}(u, \alpha) = 0 \\ H(u(0), \alpha) = 0 \\ \langle H_x(u(0), \alpha), f^{(i)}(u(0), \alpha) \rangle = 0 \\ H(u(1), \alpha) = 0 \end{cases}$	$2, 1$ 
Orbit of vector field $f^{(i)}$ connecting a pseudo-equilibrium with the boundary $\Sigma$ $\begin{cases} \dot{u} - T f^{(i)}(u, \alpha) = 0 \\ H(u(0), \alpha) = 0 \\ \lambda_i f^{(i)}(u(0), \alpha) + \lambda_j f^{(j)}(u(0), \alpha) = 0, j \neq i \\ \lambda_i + \lambda_j - 1 = 0 \\ H(u(1), \alpha) = 0 \end{cases}$	$n, 1$ 
Grazing bifurcation of vector field $f^{(i)}$ $\begin{cases} \dot{u} - T f^{(i)}(u, \alpha) = 0 \\ H(u(0), \alpha) = 0 \\ \langle H_x(u(0), \alpha), f^{(i)}(u(0), \alpha) \rangle = 0 \\ u(0) - u(1) = 0 \end{cases}$	$n, 2$ 
Orbit of vector field $f^{(i)}$ connecting two tangent points of $f^{(i)}$ $\begin{cases} \dot{u} - T f^{(i)}(u, \alpha) = 0 \\ H(u(0), \alpha) = 0 \\ \langle H_x(u(0), \alpha), f^{(i)}(u(0), \alpha) \rangle = 0 \\ H(u(1), \alpha) = 0 \\ \langle H_x(u(1), \alpha), f^{(i)}(u(1), \alpha) \rangle = 0 \end{cases}$	$2, 2$ 

Table II. (continued)

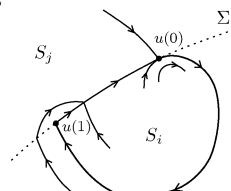
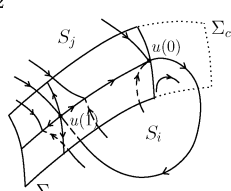
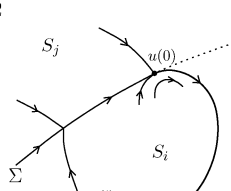
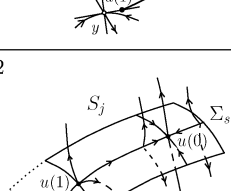
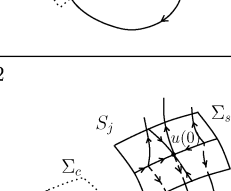
Defining System	$n, m$
Orbit of vector field $f^{(i)}$ connecting a tangent point of $f^{(i)}$ with a tangent point of $f^{(j)}$ ( $j \neq i$ ) $\left\{ \begin{array}{l} \dot{u} - Tf^{(i)}(u, \alpha) = 0 \\ H(u(0), \alpha) = 0 \\ \langle H_x(u(0), \alpha), f^{(i)}(u(0), \alpha) \rangle = 0 \\ H(u(1), \alpha) = 0 \\ \langle H_x(u(1), \alpha), f^{(j)}(u(1), \alpha) \rangle = 0 \end{array} \right.$	2, 2 
Orbit of vector field $f^{(i)}$ connecting a tangent point of $f^{(i)}$ with a pseudo-equilibrium $\left\{ \begin{array}{l} \dot{u} - Tf^{(i)}(u, \alpha) = 0 \\ H(u(0), \alpha) = 0 \\ \langle H_x(u(0), \alpha), f^{(i)}(u(0), \alpha) \rangle = 0 \\ H(u(1), \alpha) = 0 \\ \lambda_i f^{(i)}(u(1), \alpha) + \lambda_j f^{(j)}(u(1), \alpha) = 0, j \neq i \\ \lambda_i + \lambda_j - 1 = 0 \end{array} \right.$	$n, 2$ 
Orbit of vector field $f^{(i)}$ connecting a tangent point of $f^{(i)}$ to a saddle $\left\{ \begin{array}{l} \dot{u} - Tf^{(i)}(u, \alpha) = 0 \\ H(u(0), \alpha) = 0 \\ \langle H_x(u(0), \alpha), f^{(i)}(u(0), \alpha) \rangle = 0 \\ f^{(i)}(y, \alpha) = 0 \\ [f_x^{(i)}(y, \alpha)]^T w - \nu w = 0, \nu > 0 \\ \langle w, w \rangle - 1 = 0 \\ \langle w, y - u(1) \rangle = 0 \end{array} \right.$	2, 2 
Orbit of vector field $f^{(i)}$ connecting a pseudo-equilibrium with a tangent point of $f^{(i)}$ $\left\{ \begin{array}{l} \dot{u} - Tf^{(i)}(u, \alpha) = 0 \\ H(u(0), \alpha) = 0 \\ \lambda_i f^{(i)}(u(0), \alpha) + \lambda_j f^{(j)}(u(0), \alpha) = 0, j \neq i \\ \lambda_i + \lambda_j - 1 = 0 \\ H(u(1), \alpha) = 0 \\ \langle H_x(u(1), \alpha), f^{(i)}(u(1), \alpha) \rangle = 0 \end{array} \right.$	$n, 2$ 
Orbit of vector field $f^{(i)}$ connecting a pseudo-equilibrium with a tangent point of $f^{(j)}$ ( $j \neq i$ ) $\left\{ \begin{array}{l} \dot{u} - Tf^{(i)}(u, \alpha) = 0 \\ H(u(0), \alpha) = 0 \\ \lambda_i f^{(i)}(u(0), \alpha) + \lambda_j f^{(j)}(u(0), \alpha) = 0 \\ \lambda_i + \lambda_j - 1 = 0 \\ H(u(1), \alpha) = 0 \\ \langle H_x(u(1), \alpha), f^{(j)}(u(1), \alpha) \rangle = 0 \end{array} \right.$	$n, 2$ 

Table II. (continued)

Defining System	$n, m$
<p>Orbit of vector field <math>f^{(i)}</math> connecting two pseudo-equilibria</p> $\begin{cases} \dot{u} - Tf^{(i)}(u, \alpha) = 0 \\ H(u(0), \alpha) = 0 \\ \lambda_i f^{(i)}(u(0), \alpha) + \lambda_j f^{(j)}(u(0), \alpha) = 0, j \neq i \\ \lambda_i + \lambda_j - 1 = 0 \\ H(u(1), \alpha) = 0 \\ \mu_i f^{(i)}(u(1), \alpha) + \mu_j f^{(j)}(u(1), \alpha) = 0 \\ \mu_i + \mu_j - 1 = 0 \end{cases}$	<p>2, 2</p>
<p>Orbit of vector field <math>f^{(i)}</math> connecting a pseudo-equilibrium to a saddle with a one-dimensional unstable manifold</p> $\begin{cases} \dot{u} - Tf^{(i)}(u, \alpha) = 0 \\ H(u(0), \alpha) = 0 \\ \lambda_i f^{(i)}(u(0), \alpha) + \lambda_j f^{(j)}(u(0), \alpha) = 0, j \neq i \\ \lambda_i + \lambda_j - 1 = 0 \\ f^{(i)}(y, \alpha) = 0 \\ [f_x^{(i)}(y, \alpha)]^T w - \nu w = 0, \nu > 0 \\ \langle w, w \rangle - 1 = 0 \\ \langle w, y - u(1) \rangle = 0 \end{cases}$	<p><math>n, 2</math></p>

which we rewrite as

$$F(x, \alpha, \beta) = 0, \quad x \in \mathbf{R}^n, F \in \mathbf{R}^{n_d}, \alpha \in \mathbf{R}^m, \beta \in \mathbf{R}^{m_d}, \quad (6)$$

as well as paths of solutions to *boundary-value problems* with non-separated boundary conditions:

$$\dot{U}(\tau) - F(U(\tau), \alpha, \beta) = 0, \quad U, F \in \mathbf{R}^{n_d}, \alpha \in \mathbf{R}^m, \beta \in \mathbf{R}^{m_d}, \tau \in [0, 1] \quad (7a)$$

$$b(U(0), U(1), \alpha, \beta) = 0, \quad b \in \mathbf{R}^{n_b}. \quad (7b)$$

Functions  $F$  and  $b$  are assumed to be sufficiently smooth. In both cases,  $m$  control parameters,  $\alpha = (\alpha_1, \dots, \alpha_m)$ , and  $m_d$  other parameters of the defining system,  $\beta = (\beta_1, \dots, \beta_{m_d})$ , are allowed to vary, and the following conditions on dimensions are imposed:

$$n + m + m_d = n_d + 1 \quad (8a)$$

for equation (6) and

$$m + m_d = n_b - n_d + 1 \quad (8b)$$

for equations (7).

Table I lists defining systems formulated as algebraic problems, while Table II lists those formulated as boundary-value problems, along with a graphical representation (if the boundary-value problem is defined for  $n$ -dimensional systems, we illustrate it for  $n = 3$ ). All boundary-value problems involving one standard orbit segment have also been implemented in a modified form in which two standard segments compose an orbit that crosses the discontinuity

boundary  $\Sigma$  once, but the corresponding defining systems are not given in the Table II (see, however, Section 5.2 and the User Guide to SLIDECONT [Dercole and Kuznetsov 2004]).

Note that the defining systems for standard equilibrium and cycle continuation (see Tables I and II, respectively) are also not given since they correspond to AUTO97 built-in problems. Similarly, the defining systems for the continuation of pseudo-saddle-node and double tangency bifurcations (see Table I) are not given since they are implemented indirectly by using the defining systems for pseudo-equilibrium and tangent point continuation (Table I) and enabling AUTO97 limit point continuation.

For each defining system, accurate detection of additional local degeneracies along a solution branch is supported (see Section 5 and the User Guide to SLIDECONT [Dercole and Kuznetsov 2004] for details) together with options to switch between different defining systems.

As we have already mentioned, crossing periodic orbits and periodic orbits with one sliding segment are supported for general  $n$ -dimensional Filippov systems. Moreover, SLIDECONT supports detection and continuation of all codimension 1 bifurcations in planar Filippov systems, including the following bifurcations of periodic orbits: *grazing (touching)*, *switching (buckling)*, and *crossing*, as well as *sliding homoclinic orbits to saddles and pseudo-saddles* (see Kuznetsov et al. [2003]). For  $n$ -dimensional Filippov systems, both the grazing periodic orbits and the orbits connecting pseudo-equilibria with tangent points or saddles can be continued by SLIDECONT in two control parameters.

#### 4. STRUCTURE OF SLIDECONT

In this section the structure of SLIDECONT is presented, together with some comments on its implementation (which is further described in the next section and in Dercole and Kuznetsov [2004]). The overall structure of SLIDECONT is illustrated in Figure 2.

As in AUTO97, the user must provide three files: An equations file (`<name>.f`, where `<name>` is a user-selected name), a constants file (`sc.<name>`), and, in some cases, a data file (`<name>.dat`) (see Figure 2). The equations file contains a set of Fortran subroutines specifying the model (4), namely the two vector fields,  $f^{(1)}$  and  $f^{(2)}$ , and the scalar function  $H$ ; the starting solution, either analytically or numerically; and optional state and parameter user functions to be monitored during continuation. Some problems require the analytical derivatives of  $f^{(1)}$ ,  $f^{(2)}$ , and  $H$  (see Section 5 and the User Guide to SLIDECONT [Dercole and Kuznetsov 2004]). The constants file specifies all numerical parameters needed by the AUTO97 continuation algorithms, along with SLIDECONT specific constants, for example, the problem type, which defines the problem to be solved. Following AUTO97 conventions, SLIDECONT problem types are coded by integers. This is done in such a way that SLIDECONT problem types do not conflict with those built into AUTO97, so that the SLIDECONT user can access all AUTO97 facilities. For boundary-value problems, the data file numerically specifies a starting solution.

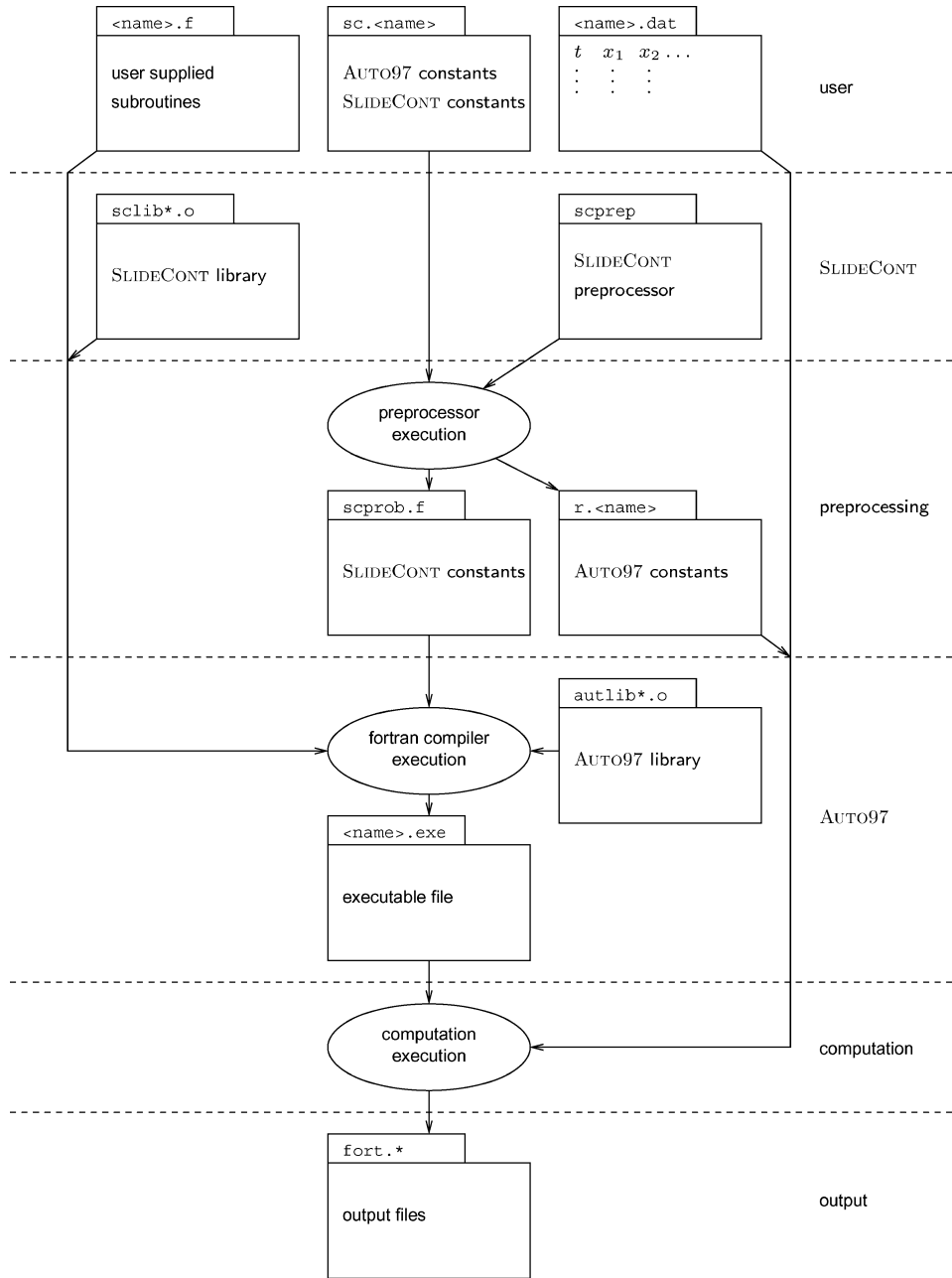


Fig. 2. SLIDECONT implementation structure.

As shown in Figure 2, SLIDECONT is composed of two parts: the SLIDECONT pre-processor (`scprep`) and the SLIDECONT library (`sclib*.o`). Preprocessing takes the user constants file and produces the corresponding AUTO97 constants file (`r.<name>`) and a problem specific Fortran file (`scprob.f`) containing an initialization subroutine, which is called by the subroutine of the SLIDECONT library first called by AUTO97. The library contains the standard AUTO97 user subroutines for each problem and additional support routines.

Compiling the user and problem-specific Fortran files and their linking with the SLIDECONT and AUTO97 libraries produces an executable file (`<name>.exe`) whose execution finally generates the standard AUTO97 output files (`fort.*`).

## 5. TWO DETAILED PROBLEM DESCRIPTIONS

In this section we describe in detail the SLIDECONT implementation of two particular defining systems: the algebraic problem for the continuation of a pseudo-equilibrium (see Table I) and the boundary-value problem for the continuation of a sliding cycle (see Table II). These two cases serve as illustrative examples; we refer to the User Guide to SLIDECONT [Dercole and Kuznetsov 2004] for all other cases listed in Tables I and II.

### 5.1 Continuation of a Pseudo-Equilibrium

The defining system for continuing a pseudo-equilibrium of (4) is given below for reference:

$$\begin{cases} H(x, \alpha) = 0, \\ \lambda_1 f^{(1)}(x, \alpha) + \lambda_2 f^{(2)}(x, \alpha) = 0, \\ \lambda_1 + \lambda_2 - 1 = 0. \end{cases} \quad (9)$$

The first equation of (9) requires that  $x$  lies on the discontinuity boundary  $\Sigma(\alpha)$ , while the second and third equations require that a convex combination of  $f^{(1)}(x, \alpha)$  and  $f^{(2)}(x, \alpha)$  vanishes. This means  $x$  is a pseudo-equilibrium of (4), that is,  $f^{(1)}(x, \alpha)$  and  $f^{(2)}(x, \alpha)$  are anti collinear, only if  $\lambda_1$  and  $\lambda_2$  have the same sign.

Referring back to Equation (6), the defining system (9) is composed of  $n_d = n + 2$  scalar equations and is defined in the  $(m + 2)$ -dimensional parameter space  $(\alpha, \lambda_1, \lambda_2)$  (i.e.,  $m_d = 2$  and  $\beta = (\lambda_1, \lambda_2)$ ). It then follows from condition (8a) that  $m = 1$ , that is, pseudo-equilibria can be generically continued with respect to one control parameter.

Some implementation details are given in Table III using AUTO97 notation. In particular: `IPS` is the AUTO97 problem type (`IPS=0` corresponds to algebraic problems, see AUTO97 documentation); `SCIDIFF` is the order up to which analytical derivatives of  $f^{(1)}$ ,  $f^{(2)}$ , and  $H$  are required; `NDIM` is the problem dimension; `U(1), ..., U(NDIM)` and `F(1), ..., F(NDIM)` specify the composition of the vectors  $U$  and  $F$  of Equation (5); `NICP` is the total number of parameters allowed to vary and `ICP(1), ..., ICP(NICP)` is the list of their indexes in the parameter vector `PAR`, assuming `PAR(i) = \alpha_i` and reporting the parameter

Table III. Implementation Details of the Algebraic Problem (9)

$n, m$	$n, 1$
$m_d, (\beta_1, \dots, \beta_{m_d})$	$2, (\lambda_1, \lambda_2)$
$n_d$	$n + 2$
IPS, SCIDIFF, NDIM	$0, 0, n + 2$
$U(1), \dots, U(\text{NDIM})$	$x_1, \dots, x_n, \lambda_1, \lambda_2$
$F(k), k = 1, \dots, n$	$\lambda_1 f_k^{(1)}(x, \alpha) + \lambda_2 f_k^{(2)}(x, \alpha)$
$F(n + 1)$	$H(x, \alpha)$
$F(n + 2)$	$\lambda_1 + \lambda_2 - 1$
NICP, (ICP(1), $\dots$ , ICP(NICP))	$1, (1(\alpha))$
t.f.1: boundary equilibrium of $f^{(1)}$	$\lambda_2$
t.f.2: boundary equilibrium of $f^{(2)}$	$\lambda_1$
t.f.3: singular sliding point	$\langle H_x(x, \alpha), f^{(1)}(x, \alpha) \rangle$
t.f.: pseudo-saddle-node bifurcation	AUTO97 limit point

symbol in parenthesis next to the corresponding index. Table III also lists the test functions available for detecting additional local degeneracies (see Dercole and Kuznetsov [2004] for the list of all possible switches to different defining systems).

## 5.2 Continuation of a Sliding Cycle

In this subsection we focus on the continuation of solutions of (4) composed of standard and sliding segments. We consider the most relevant case of periodic solutions (sliding cycles), but the same approach can easily be adapted to more general solutions.

The continuation of sliding segments seems to require solving certain boundary-value problems for

$$\begin{cases} \dot{x} = g(x, \alpha), \\ 0 = H(x, \alpha). \end{cases} \quad (10)$$

Note that formally (10) is a *differential-algebraic system* for which boundary-value problem solvers are hard to develop (see, however, Ascher and Spiteri [1994]).

The crucial observation is that the Filippov vector field  $g(x, \alpha)$  defined in Section 2 can be extended from the discontinuity boundary  $\Sigma_s(\alpha)$  to its neighborhood in  $\mathbf{R}^n$ . For this *extended Filippov vector field*, all level sets  $H(x, \alpha) = h$  with small  $|h|$  and, in particular, the zero-level set  $\Sigma_s(\alpha)$  are invariant. The continuation of sliding segments can thus be carried out by setting up proper boundary-value problems for the extended Filippov vector field  $g(x, \alpha)$  with a boundary condition requiring that the solution start- or endpoint lies on  $\Sigma_s(\alpha)$ . Since  $\Sigma_s(\alpha)$  is invariant for  $g(x, \alpha)$ , the condition  $H(x(t), \alpha) = 0$  is automatically satisfied for all intermediate points of the sliding segment. This obviates any need to use boundary-value problem solvers for the differential-algebraic systems.

The defining system for the continuation of the simplest sliding cycle—a sliding cycle composed of one standard segment and one sliding segment (see

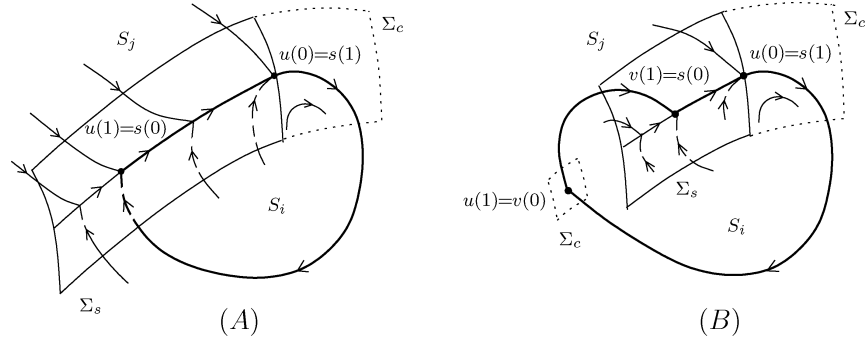


Fig. 3. Graphical representation for  $n = 3$  of (A) boundary-value problem (11) and (B) boundary-value problem (12).

Figure 2(A)—is

$$\left\{ \begin{array}{l} \dot{u} - T_i f^{(i)}(u, \alpha) = 0, \\ \dot{s} - T_0 g(s, \alpha) = 0, \\ H(u(0), \alpha) = 0, \\ \langle H_x(u(0), \alpha), f^{(i)}(u(0), \alpha) \rangle = 0, \\ s(0) - u(1) = 0, \\ s(1) - u(0) = 0, \end{array} \right. \quad (11)$$

where  $T_i$  and  $T_0$  are parameters meaning the time spent by the  $(T_i + T_0)$ -periodic solution of (4) in region  $S_i$  and on  $\Sigma(\alpha)$ , respectively. The boundary conditions  $s(0) = u(1)$  and  $s(1) = u(0)$  ensure the periodicity, while the two scalar conditions involving  $H$  force the start-point of the standard solution  $u(0)$  to be a visible tangent point of vector field  $f^{(i)}$  (see Figure 2(A)). The first scalar condition also implies that the endpoint of the sliding solution  $s(1)$  lies on  $\Sigma_s(\alpha)$ , along with the entire sliding segment. The complete periodic solution is then given by

$$x(t) = \begin{cases} u\left(\frac{t}{T_i}\right), & t \in [0, T_i], \\ s\left(\frac{t - T_i}{T_0}\right), & t \in [T_i, T_i + T_0]. \end{cases}$$

Analogously, the following boundary-value problem can be used to continue a sliding cycle composed of two standard segments and one sliding segment (see Figure 2(B)):

$$\left\{ \begin{array}{l} \dot{u} - T_i f^{(i)}(u, \alpha) = 0, \\ \dot{v} - T_j f^{(j)}(v, \alpha) = 0, \\ \dot{s} - T_0 g(s, \alpha) = 0, \\ H(u(0), \alpha) = 0, \\ \langle H_x(u(0), \alpha), f^{(i)}(u(0), \alpha) \rangle = 0, \\ H(u(1), \alpha) = 0, \\ v(0) - u(1) = 0, \\ s(0) - v(1) = 0, \\ s(1) - u(0) = 0, \end{array} \right. \quad (12)$$

Table IV. Implementation Details of the Boundary-Value Problem (11)

$n, m$	$n, 1$
$m_d, (\beta_1, \dots, \beta_{m_d})$	$2, (T_i, T_0)$
$n_d, n_b$	$2n, 2n + 2$
IPS, SCIDIFF, NDIM, NBC	$4, 1, 2n, 2n + 2$
$U(1), \dots, U(\text{NDIM})$	$u_1, \dots, u_n, s_1, \dots, s_n$
$F(k), k = 1, \dots, n$	$T_i f_k^{(i)}(u, \alpha)$
$F(k), k = n + 1, \dots, 2n$	$T_0 g(s, \alpha)$
NICP, (ICP(1), $\dots$ , ICP(NICP))	$3, (1(\alpha), 60(T_s), 61(T_i))$
t. f. 1: boundary equilibrium of $f^{(i)}$ at $u(0)$ ( $n = 2$ )	$\langle (H_{x_2}(u(0), \alpha), -H_{x_1}(u(0), \alpha)), f^{(i)}(u(0), \alpha) \rangle$
t. f. 2: tangent point of $f^{(j)}$ at $u(0)$	$\langle H_x(u(0), \alpha), f^{(j)}(u(0), \alpha) \rangle$
t. f. 3: tangent point of $f^{(i)}$ at $u(1)$	$\langle H_x(u(1), \alpha), f^{(i)}(u(1), \alpha) \rangle$
t. f. 4: tangent point of $f^{(j)}$ at $u(1)$	$\langle H_x(u(1), \alpha), f^{(j)}(u(1), \alpha) \rangle$
t. f. 5: pseudo-equilibrium at $u(1)$ ( $n = 2$ )	$\langle (H_{x_2}(u(1), \alpha), -H_{x_1}(u(1), \alpha)), g(u(1), \alpha) \rangle$

and the corresponding  $(T_i + T_j + T_0)$ -periodic solution of (4) is given by

$$x(t) = \begin{cases} u\left(\frac{t}{T_i}\right), & t \in [0, T_i], \\ v\left(\frac{t - T_i}{T_j}\right), & t \in [T_i, T_i + T_j], \\ s\left(\frac{t - (T_i + T_j)}{T_0}\right), & t \in [T_i + T_j, T_i + T_j + T_0]. \end{cases}$$

With reference to equations (7), the defining system (11) is comprised of  $n_d = 2n$  differential equations and  $n_b = 2n + 2$  boundary conditions, counted as scalar equations, and is defined in the  $(m + 2)$ -dimensional parameter space  $(\alpha, T_i, T_0)$ ,  $m_d = 2$  and  $\beta = (T_i, T_0)$ . For the defining system (12),  $n_d = 3n$ ,  $n_b = 3n + 3$ , and the parameter space  $(\alpha, T_i, T_j, T_0)$  is  $(m + 3)$ -dimensional,  $m_d = 3$  and  $\beta = (T_i, T_j, T_0)$ . In both cases, condition (8b) implies  $m = 1$ , meaning that sliding cycles can be generically continued with respect to one control parameter.

Tables IV and V report implementation details analogous to those reported in Table III.

## 6. EXAMPLES

We now describe three of the examples distributed with SLIDECONT, each of which involves several computations supported by SLIDECONT. Throughout the description, the stability of particular solutions has been inferred from numerical integration. To execute all prepared computations, the user can simply enter make in the corresponding example directory, or use SLIDECONT commands to execute each computation separately (see the User Guide to SLIDECONT).

### 6.1 Simple Dry Friction Oscillations

Consider a linear damped oscillator with dry friction:

$$\dot{x}_1 + x_1 = \alpha_1 \alpha_3 \text{sgn}(\alpha_5 - \dot{x}_1) - \alpha_2 \alpha_4 (\alpha_5 - \dot{x}_1) \quad (13)$$

Table V. Implementation Details of the Boundary-Value Problem (12)

$n, m$	$n, 1$
$m_d, (\beta_1, \dots, \beta_{m_d})$	$2, (T_i, T_j, T_0)$
$n_d, n_b$	$3n, 3n + 3$
IPS, SCIDIFF, NDIM, NBC	$4, 1, 3n, 3n + 3$
$U(1), \dots, U(\text{NDIM})$	$u_1, \dots, u_n, v_1, \dots, v_n, s_1, \dots, s_n$
$F(k), k = 1, \dots, n$	$T_i f_k^{(i)}(u, \alpha)$
$F(k), k = n + 1, \dots, 2n$	$T_j f_k^{(j)}(u, \alpha)$
$F(k), k = 2n + 1, \dots, 3n$	$T_0 g(s, \alpha)$
NICP, (ICP(1), ..., ICP(NICP))	$4, (1(\alpha), 60(T_s), 61(T_i), 62(T_j))$
t. f. 1: boundary equilibrium of $f^{(i)}$ at $u(0)$ ( $n = 2$ )	$\langle (H_{x_2}(u(0), \alpha), -H_{x_1}(u(0), \alpha)), f^{(i)}(u(0), \alpha) \rangle$
t. f. 2: tangent point of $f^{(j)}$ at $u(0)$	$\langle H_x(u(0), \alpha), f^{(j)}(u(0), \alpha) \rangle$
t. f. 3: tangent point of $f^{(i)}$ at $u(1)$	$\langle H_x(u(1), \alpha), f^{(i)}(u(1), \alpha) \rangle$
t. f. 4: tangent point of $f^{(j)}$ at $u(1)$	$\langle H_x(u(1), \alpha), f^{(j)}(u(1), \alpha) \rangle$
t. f. 5: tangent point of $f^{(i)}$ at $v(1)$	$\langle H_x(v(1), \alpha), f^{(i)}(v(1), \alpha) \rangle$
t. f. 6: tangent point of $f^{(j)}$ at $v(1)$	$\langle H_x(v(1), \alpha), f^{(j)}(v(1), \alpha) \rangle$
t. f. 7: pseudo-equilibrium at $v(1)$ ( $n = 2$ )	$\langle (H_{x_2}(v(1), \alpha), -H_{x_1}(v(1), \alpha)), g(v(1), \alpha) \rangle$

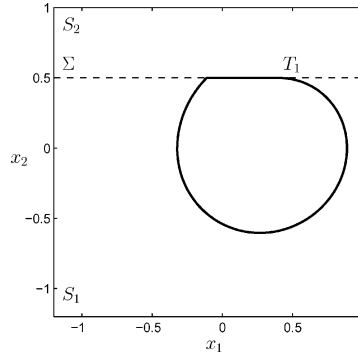


Fig. 4. A sliding cycle in (13).

(see, for example, Tondl [1970]). This defines a piecewise-linear Filippov system (4) with  $x_2 = \dot{x}_1$ ,  $H(x, \alpha) = x_2 - \alpha_5$ ,

$$S_1 = \{x \in \mathbf{R}^2 : x_2 - \alpha_5 < 0\}, \quad S_2 = \{x \in \mathbf{R}^2 : x_2 - \alpha_5 > 0\}$$

and

$$f^{(1,2)}(x) = \begin{pmatrix} x_2 \\ -x_1 \pm \alpha_1 \alpha_3 - \alpha_2 \alpha_4 (\alpha_5 - x_2) \end{pmatrix}.$$

Set

$$\alpha_1 = 0.1, \alpha_2 = 0.03, \alpha_3 = \alpha_4 = 4, \alpha_5 = 0.5.$$

At these parameter values the system has a stable sliding cycle that starts at the visible tangent point  $T_1$  of  $f^{(1)}$  and is composed of a standard segment in  $S_1$  and a horizontal sliding segment (see Figure 4). Data files containing the initial solutions to the boundary-value problem (11) can be easily produced by numerically integrating the vector field  $f^{(1)}$  and the Filippov vector field  $g$  (see Equation (2)).

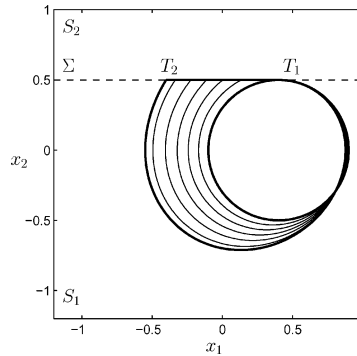


Fig. 5. Continuation of the sliding cycle of (13) with respect to  $\alpha_2$ . The thick solutions correspond to a grazing bifurcation at  $\alpha_2 = 0$  and a switching bifurcation at  $\alpha_2 = \alpha_2^{sw}$ .

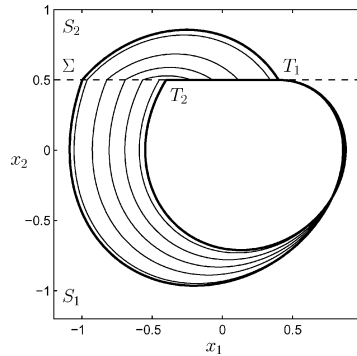


Fig. 6. Continuation of the sliding cycle of (13) for increasing values of  $\alpha_2$ . The thick solutions correspond to the switching bifurcation at  $\alpha_2 = \alpha_2^{sw}$  and a crossing bifurcation at  $\alpha_2 = \alpha_2^{cc}$ .

First we use the boundary-value problem (11) to continue the sliding cycle of Figure 4 with respect to  $\alpha_2$ . The result is shown in Figure 5. The solution family ends on one side at  $\alpha_2 = 0$  in a grazing bifurcation (test function 3 vanishes, see Table IV). This bifurcation is degenerate since at  $\alpha_2 = 0$  the systems in both  $S_1$  and  $S_2$  become linear oscillators with closed orbits around  $(\alpha_1\alpha_3, 0)$  and  $(-\alpha_1\alpha_3, 0)$ , respectively (portrait *O* in Figure 8). On the other side, the solution family ends at  $\alpha_2^{sw} = 0.0557\dots$  in a switching bifurcation: an invisible tangent point  $T_2$  of  $f^{(2)}$  is detected at the end point  $u(1)$  as zero of test function 4 (see Figures 5 and 8(SW) and Table IV).

For  $\alpha_2$  slightly larger than  $\alpha_2^{sw}$ , the sliding cycles also have a standard segment in  $S_2$  (portrait **2** in Figure 8) and can therefore be continued by means of the boundary-value problem (12). The result is shown in Figure 6. The solution family ends at  $\alpha_2^{cc} = 0.1023\dots$  in a crossing bifurcation: the visible tangent point  $T_1$  of  $f^{(1)}$  is detected at the end point  $v(1)$  as zero of test function 5 (see Figures 6 and 8(CC) and Table V)—the sliding segment vanishes. According to Kuznetsov et al. [2003], this implies that a *stable crossing cycle* replaces the sliding cycle for  $\alpha_2$  slightly larger than  $\alpha_2^{cc}$ .

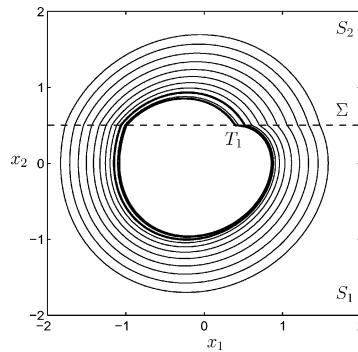


Fig. 7. A family of crossing cycles of (13). The thick solutions correspond to a fold bifurcation of crossing cycles at  $\alpha_2 = \alpha_2^{lp}$  and the crossing bifurcation at  $\alpha_2 = \alpha_2^{cc}$ .

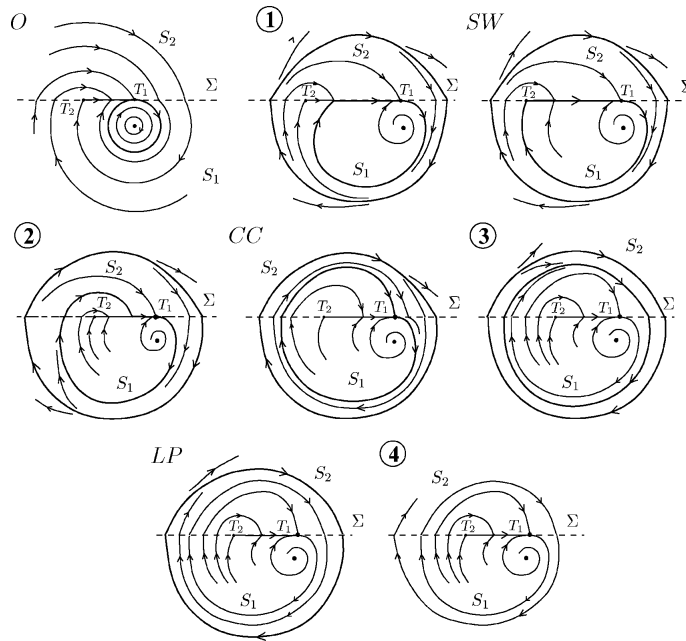


Fig. 8. Bifurcation diagram of (13): *O*—centers ( $\alpha_2 = 0$ ); **1**—a sliding cycle with the standard arc in  $S_1$  and a crossing cycle ( $0 < \alpha_2 < \alpha_2^{sw}$ ); *SW*—switching bifurcation at  $\alpha_2 = \alpha_2^{sw}$ ; **2**—a sliding cycle with the standard arcs in both  $S_1$  and  $S_2$  and a crossing cycle ( $\alpha_2^{sw} < \alpha_2 < \alpha_2^{cc}$ ); *CC*—crossing bifurcation at  $\alpha_2 = \alpha_2^{cc}$ ; **3**—two crossing cycles ( $\alpha_2^{cc} < \alpha_2 < \alpha_2^{lp}$ ); *LP*—limit point of the crossing cycles at  $\alpha_2 = \alpha_2^{lp}$ ; **4**—no attractors ( $\alpha_2 > \alpha_2^{lp}$ ).

Numerical integration backward in time at  $\alpha_2 = 0.0716$ , however, reveals an unstable crossing cycle, which can be continued for increasing values of  $\alpha_2$  (see Table II). The result is shown graphically in Figure 7. A *fold bifurcation of crossing cycles* is detected at  $\alpha_2^{lp} = 0.1044 \dots$ , where the unstable crossing cycle collides with the stable inner crossing cycle (born at the crossing bifurcation at  $\alpha_2^{cc}$ ) and disappears via the fold bifurcation (Figure 8(*LP*)).

Figure 7 shows the stable inner crossing cycles of the solution family born at the fold bifurcation, for values of  $\alpha_2$  decreasing to  $\alpha_2^{cc}$ , at which the crossing bifurcation occurs. The unstable crossing cycle exists for all  $\alpha_2$  satisfying  $0 < \alpha_2 < \alpha_2^{lp}$  (see portraits **1**, *SW*, **2**, *CC*, and **3** in Figure 8), and its amplitude grows to infinity as  $\alpha_2 \rightarrow 0$ . No periodic motion is present above the critical parameter value  $\alpha_2^{lp}$  (portrait **4** in Figure 8). Thus, the construction of the one-parameter bifurcation diagram of (13) is complete.

## 6.2 Forced Dry Friction Oscillations

As an example of two-parameter continuation of grazing cycles in a 4-dimensional Filippov system, consider a dry friction oscillator described by the equation

$$\dot{x}_1 + x_1 = \alpha_1 \operatorname{sgn}(1 - \dot{x}_1) - \alpha_2(1 - \dot{x}_1) + \alpha_3(1 - \dot{x}_1)^3 + \alpha_4 \cos(\alpha_5 t) \quad (14)$$

[Yoshitake and Sueoka 2002; di Bernardo et al. 2003]. Here positive constants  $\alpha_1, \alpha_2, \alpha_3$  are the coefficients of the kinematic friction characteristics,  $\alpha_4$  is the amplitude of the forcing and  $\alpha_5$  is its angular frequency. Since  $\cos(\alpha_5 t)$  is the  $x_3$ -component of a stable periodic solution to the planar system

$$\begin{cases} \dot{x}_3 = x_3 - \alpha_5 x_4 - x_3(x_3^2 + x_4^2), \\ \dot{x}_4 = \alpha_5 x_3 + x_4 - x_4(x_3^2 + x_4^2), \end{cases}$$

Equation (14) is equivalent to a 4-dimensional Filippov system (4) with

$$f^{(1,2)}(x, \alpha) = \begin{pmatrix} x_2 \\ -x_1 \pm \alpha_1 - \alpha_2(1 - x_2) + \alpha_3(1 - x_2)^3 + \alpha_4 x_3 \\ x_3 - \alpha_5 x_4 - x_3(x_3^2 + x_4^2) \\ \alpha_5 x_3 + x_4 - x_4(x_3^2 + x_4^2) \end{pmatrix},$$

and

$$H(x, \alpha) = x_2 - 1.$$

Embedding an  $n$ -dimensional harmonically forced system into an autonomous  $(n + 2)$ -dimensional system, as done here, is routinely used in AUTO97 demos.

It is known (see [di Bernardo et al. 2003]) that at

$$\alpha_1 = \alpha_2 = 1.5, \alpha_3 = 0.45, \alpha_4 = 0.1, \alpha_5 = 1.7078 \dots$$

a  $\frac{8\pi}{\alpha_5}$ -cycle in region  $S_1$  touches the discontinuity boundary  $\Sigma$  (see Figure 9). This is a grazing bifurcation of the system. Starting with the numerical solution corresponding to Figure 9, we continue this bifurcation in two control parameters:  $\alpha_4$  and  $\alpha_5$  (see Table II). The computed family of  $\frac{8\pi}{\alpha_5}$ -periodic grazing cycles is shown in Figure 10, and the corresponding bifurcation curve  $TCH_2$  in the  $(\alpha_4, \alpha_5)$  plane is presented in Figure 11.

The solution at point  $A_1 = (\alpha_4, \alpha_5) = (1.3242\dots, 2.5481\dots)$  is close to a grazing solution with period  $\frac{4\pi}{\alpha_5}$  that is traced twice: the grazing cycle undergoes a period-halving bifurcation that is detected by SLIDECONT as a *branch point*. In other words, the periodically forced dry friction oscillator exhibits a codimension-2 bifurcation when a nonhyperbolic  $\frac{4\pi}{\alpha_5}$ -cycle touches

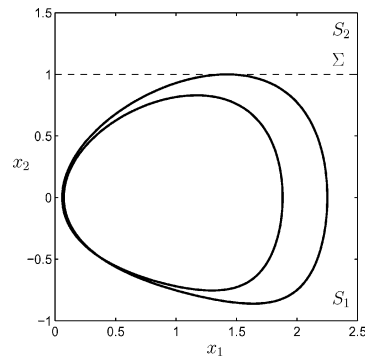


Fig. 9. A grazing cycle of the periodically forced dry friction oscillator (14).

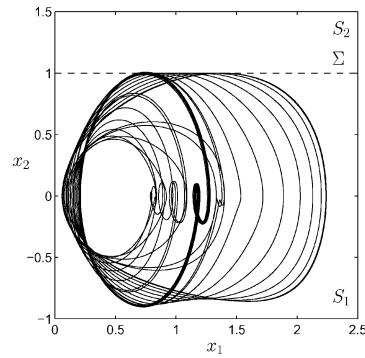


Fig. 10. A family of  $\frac{8\pi}{\alpha_5}$ -periodic grazing cycles terminating in a period-halving bifurcation at  $A_1$ , where the corresponding solution (thick orbit) is traced twice.

the discontinuity boundary at  $A_1$ . (There are two flip (period-doubling) bifurcations of the  $\frac{8\pi}{\alpha_5}$ -periodic grazing cycle at some points in the computed branch. These additional codimension-2 flip-grazing points are not shown in Figure 11.)

Continuing the grazing bifurcation of the  $\frac{4\pi}{\alpha_5}$ -cycle requires a data file that can be constructed manually from the output at the branch point or obtained by numerical integration. The computed family of  $\frac{4\pi}{\alpha_5}$ -periodic grazing cycles is shown in Figure 12. The corresponding bifurcation curve  $TCH_1$  in the  $(\alpha_4, \alpha_5)$  plane can be seen in Figure 11. Note that the flip-grazing point  $A_1$  is detected again as a flip bifurcation of the  $\frac{4\pi}{\alpha_5}$ -periodic grazing cycle, and that another branch point is detected at  $A_2 = (\alpha_4, \alpha_5) = (2.8142\dots, 3.0345\dots)$ , where the grazing cycle undergoes a period-halving bifurcation.

Finally, the curve  $PD_1$  emanating from point  $A_1$  in Figure 11 corresponds to the flip bifurcation of the  $\frac{4\pi}{\alpha_5}$ -cycle. This curve is obtained by switching to flip continuation at the point  $A_1$  detected on  $TCH_1$ .

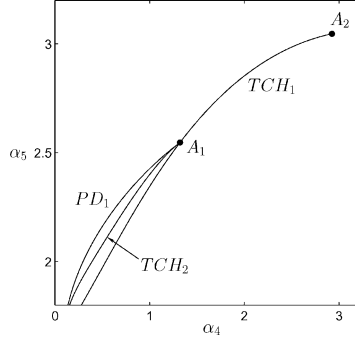


Fig. 11. Bifurcation curves of (14):  $TCH_1$ —grazing bifurcation of the  $\frac{4\pi}{\alpha_5}$ -cycle;  $PD_1$ —flip bifurcation of the  $\frac{4\pi}{\alpha_5}$ -cycle;  $TCH_2$ —grazing bifurcation of the  $\frac{8\pi}{\alpha_5}$ -cycle;  $A_{1,2}$ —codimension-2 flip-grazing points.

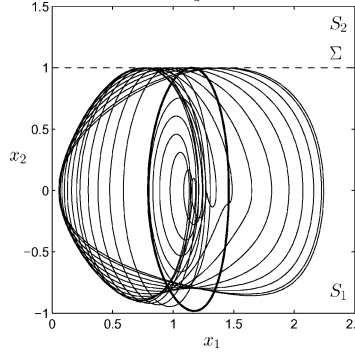


Fig. 12. A family of  $\frac{4\pi}{\alpha_5}$ -periodic grazing cycles terminating in a period-halving bifurcation at  $A_2$ , where the corresponding solution (thick orbit) is traced twice.

### 6.3 Harvesting a Prey-Predator Community

System (4) with

$$f^{(1)}(x, \alpha) = \begin{pmatrix} x_1(1 - x_1) - \psi(x_1)x_2 \\ \psi(x_1)x_2 - \alpha_3x_2 \end{pmatrix}, \tag{15a}$$

$$f^{(2)}(x, \alpha) = \begin{pmatrix} x_1(1 - x_1) - \psi(x_1)x_2 \\ \psi(x_1)x_2 - \alpha_3x_2 - \alpha_4x_2 \end{pmatrix}, \tag{15b}$$

$$\psi(x_1) = \frac{\alpha_1x_1}{\alpha_2 + x_1}, \tag{15c}$$

$$H(x, \alpha) = x_2 - \alpha_5. \tag{15d}$$

models a harvested prey-predator community where  $x_1$  and  $x_2$  are prey and predator population densities and harvesting of the predator population occurs at constant effort ( $\alpha_4$ ) only when predators are sufficiently abundant (i.e., if  $x_2 > \alpha_5$ ); for more details see Kuznetsov et al. [2003]; Dercole et al. [2003].

The analysis is performed with respect to  $\alpha_2$  and  $\alpha_5$  (other parameter values:  $\alpha_1 = 0.3556$ ,  $\alpha_3 = 0.0444$ ,  $\alpha_4 = 0.2067$ ) and is described in great detail in

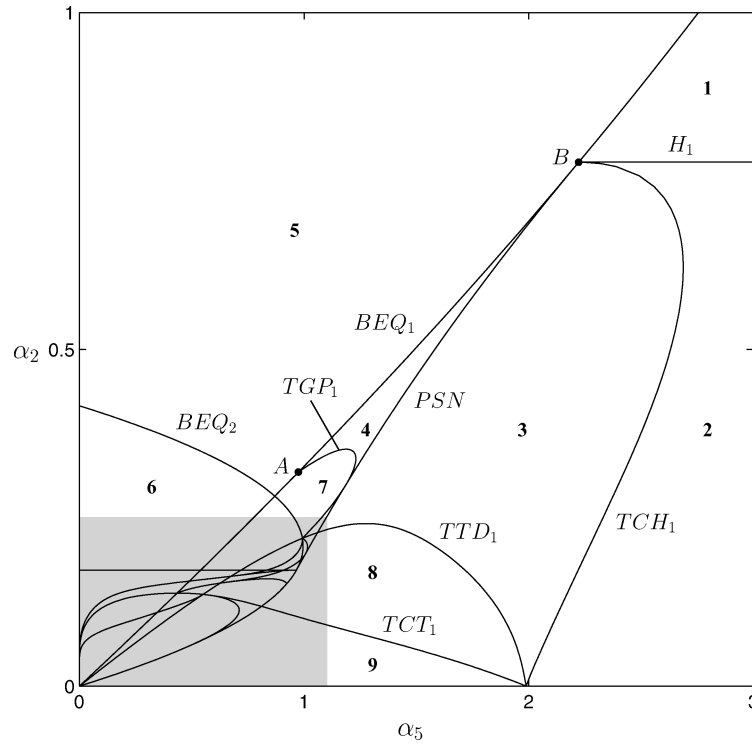


Fig. 13. Bifurcation diagram of (15) in the  $(\alpha_5, \alpha_2)$ -plane. Bifurcation curves:  $BEQ_{1,2}$ — boundary equilibrium of vector field  $f^{(1,2)}$ ;  $PSN$ —pseudo-saddle-node bifurcation;  $TCH_1$ —grazing bifurcation of vector field  $f^{(1)}$ ;  $TCT_1$ —crossing orbit of vector fields  $f^{(1)}, f^{(2)}$  connecting two tangent points of  $f^{(1)}$  (crossing bifurcation);  $TTD_1$ —orbit of vector field  $f^{(1)}$  connecting a tangent point of  $f^{(1)}$  with a tangent point of  $f^{(2)}$  (switching bifurcation);  $TGP_1$ —orbit of vector field  $f^{(1)}$  connecting a tangent point of  $f^{(1)}$  with a pseudo-equilibrium (sliding homoclinic orbit to a pseudo-saddle);  $H_1$ —Hopf bifurcation of vector field  $f^{(1)}$ ; Points  $A$  and  $B$  are codimension-2 bifurcation points detected by SLIDECONT; their coordinates are given in Table VI.

the User Guide to SLIDECONT [Dercole and Kuznetsov 2004]. The computed bifurcation curves are shown in Figures 13 and 14, and schematic state portraits corresponding to parameter regions are sketched in Figure 15. The approximate coordinates of codimension-2 points automatically detected by SLIDECONT are given in Table VI.

## 7. CONCLUSIONS AND FUTURE WORK

In this article, we have presented SLIDECONT, a new software package for sliding bifurcation analysis of Filippov systems based on AUTO97. There are several directions in which this work could be extended. First of all, there are interesting global sliding bifurcations in  $n$ -dimensional ( $n > 2$ ) Filippov systems that involve multiple sliding and which are therefore unsupported in SLIDECONT 2.0. For the planar case ( $n = 2$ ), further efforts are needed to implement more systematic detection of codimension 2 local and global bifurcations and branch switching at such bifurcations.

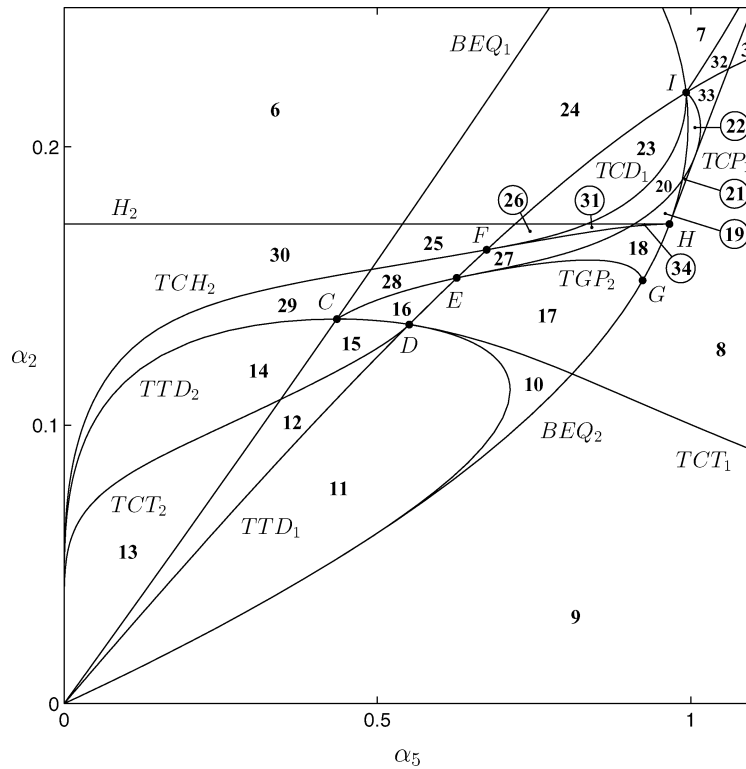


Fig. 14. Magnified view of the shaded region in Figure 13. Bifurcation curves:  $TCH_2$ —grazing bifurcation of vector field  $f^{(2)}$ ;  $TCT_2$ —crossing orbit of vector fields  $f^{(2)}$ ,  $f^{(1)}$  connecting two tangent points of  $f^{(2)}$  (crossing bifurcation);  $TTD_2$ —orbit of vector field  $f^{(2)}$  connecting a tangent point of  $f^{(2)}$  with a tangent point of  $f^{(1)}$  (switching bifurcation);  $TCD_1$ —crossing orbit of vector fields  $f^{(1)}$ ,  $f^{(2)}$  connecting a tangent point of  $f^{(1)}$  with a tangent point of  $f^{(2)}$ ;  $TGP_2$ —orbit of vector field  $f^{(2)}$  connecting a tangent point of  $f^{(2)}$  with a pseudo-equilibrium (sliding homoclinic orbit to a pseudo-saddle);  $TCP_1$ —crossing orbit of vector fields  $f^{(1)}$ ,  $f^{(2)}$  connecting a tangent point of  $f^{(1)}$  with a pseudo-equilibrium;  $H_2$ —Hopf bifurcation of vector field  $f^{(2)}$ . Other curves are the continuations of the curves from Figure 13. Points  $C - I$  are codimension-2 bifurcation points detected by SLIDECONT; their coordinates are given in Table VI.

The current version 2.0 of SLIDECONT has two major limitations. The first is related to the fact that an orbit of a Filippov system might cross the discontinuity boundary  $p$  times and involve  $q$  sliding segments. The continuation of a corresponding solution in AUTO97 would require a boundary-value problem with  $(p + 1 + q)n$  differential equations, a number which is not determined a priori. One way of allowing the continuation of a generic solution is the automatic generation of the defining system at run-time, a feature that has not yet been implemented. However, as a partial remedy to this limitation, all boundary-value problems involving only one standard segment have also been implemented in a modified form, with two standard segments (one in  $S_1$  and the other in  $S_2$ ) concatenated at the discontinuity boundary  $\Sigma$ .

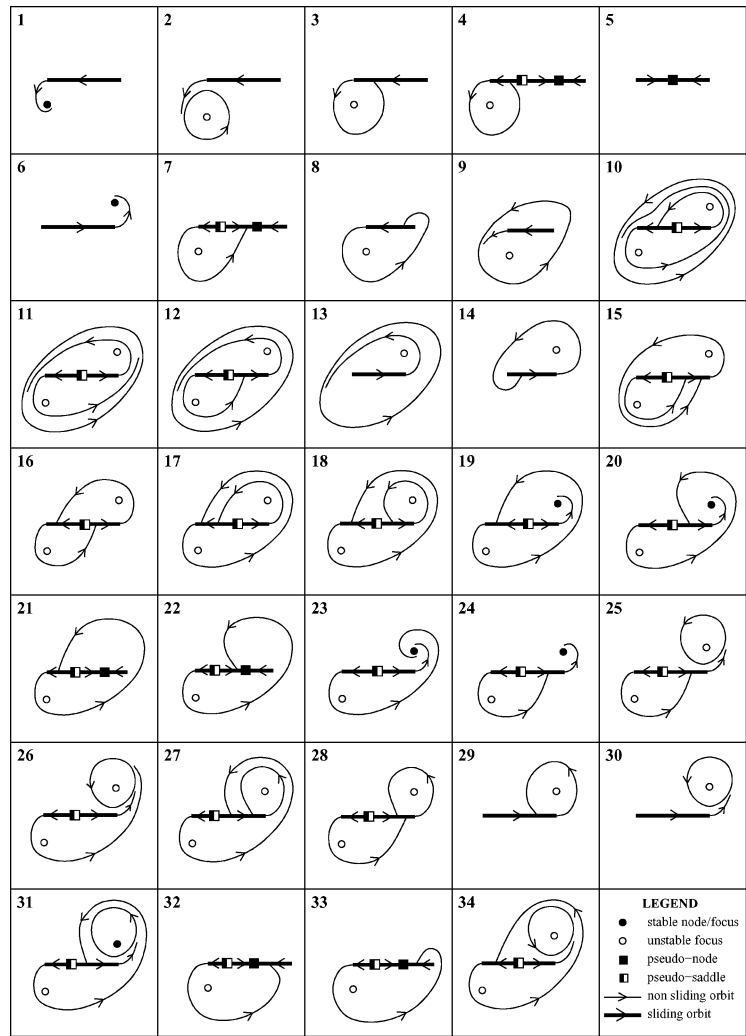


Fig. 15. Schematic phase portraits corresponding to the labeled parameter regions in Figures 13 and 14.

Table VI. Codimension 2 Points in System (15) Detected by SLIDECONT

Point	$\alpha_5$	$\alpha_2$
A	0.9747 ...	0.3177 ...
B	2.2225 ...	0.7780 ...
C	0.4352 ...	0.1381 ...
D	0.5508 ...	0.1362 ...
E	0.6266 ...	0.1529 ...
F	0.6744 ...	0.1630 ...
G	0.9232 ...	0.1519 ...
H	0.9660 ...	0.1722 ...
I	0.9925 ...	0.2195 ...

The second limitation, which will be also removed in forthcoming versions of SLIDECONT, is that the stability of pseudo-equilibria and sliding and crossing cycles is not computed. However, limit and branch points are detected by AUTO97 along a solution branch, and limit points can be continued with one extra control parameter. Note that in planar Filippov systems, periodic solutions with a stable sliding segment are always superstable (i.e., have zero multiplier).

It should also be noted that SLIDECONT does not support time-integration of Filippov systems. Such integration should be based on automatic switching from the computation of an orbit of  $f^{(i)}$  to the integration of the system (3) or its modification, and back.

Finally, SLIDECONT runs only in command mode of AUTO97 and has no GUI. The development of a software system that supports all of the above-mentioned computational tasks for  $n$ -dimensional Filippov systems in one integrated user-friendly graphic environment is another (admittedly ambitious) goal of future work.

#### ACKNOWLEDGMENTS

We are grateful to S. Rinaldi and to E. Sherwood for useful suggestions and comments on an early draft of this manuscript, and to A. Gragnani for her help in the analysis of the ecological example. We also thank E. Doedel and O. De Feo for their assistance with technical issues in AUTO97.

#### REFERENCES

- ASCHER, U. AND SPITERI, R. 1994. Collocation software for boundary value differential-algebraic equations. *SIAM J. Sci. Comput.* 15, 938–952.
- DERCOLE, F., GRAGNANI, A., KUZNETSOV, YU. A., AND RINALDI, S. 2003. Numerical sliding bifurcation analysis: An application to a relay control system. *IEEE Trans. Circuits Systems I Fund. Theory Appl.* 50, 1058–1063.
- DERCOLE, F. AND KUZNETSOV, YU. A. 2002. SLIDECONT: An AUTO97 driver for sliding bifurcation analysis. Preprint nr. 1261, Department of Mathematics, Utrecht University, The Netherlands.
- DERCOLE, F. AND KUZNETSOV, YU. A. 2004. User Guide to SLIDECONT 2.0, Department of Mathematics, Utrecht University, The Netherlands. <http://www.math.uu.nl/people/kuznet/cm/slidecont.pdf>.
- DI BERNARDO, M., BUDD, C., AND CHAMPNEYS, A. 2001. Unified framework for the analysis of grazing and border-collision in piecewise-smooth systems. *Physical Review Letters* 86, 2554–2556.
- DI BERNARDO, M., CHAMPNEYS, A., AND BUDD, C. 1998a. Grazing, skipping and sliding: analysis of the nonsmooth dynamics of the DC/DC buck converter. *Nonlinearity* 11, 858–890.
- DI BERNARDO, M., FEIGIN, M. I., HOGAN, S., AND HOMER, M. 1999. Local analysis of C-bifurcations in  $n$ -dimensional piecewise smooth dynamical systems. *Chaos, Solitons and Fractals* 10, 1881–1908.
- DI BERNARDO, M., GAROFALO, F., GLIELMO, L., AND VASCA, F. 1998b. Switchings, bifurcations and chaos in DC/DC converters. *IEEE Trans. Circuits Systems I Fund. Theory Appl.* 45, 133–141.
- DI BERNARDO, M., KOWALCZYK, P., AND NORDMARK, A. 2002. Bifurcations of dynamical systems with sliding: Derivation of normal-form mappings. *Physica D* 11, 175–205.
- DI BERNARDO, M., KOWALCZYK, P., AND NORDMARK, A. 2003. Sliding bifurcations: A novel mechanism for the sudden onset of chaos in dry-friction oscillators. *Int. J. Bifurcation and Chaos* 13, 2935–2948.
- DOEDEL, E., CHAMPNEYS, A., FAIRGRIEVE, T., KUZNETSOV, YU. A., SANDSTEDTE, B., AND WANG, X. 1997. AUTO97: Continuation and Bifurcation Software for Ordinary Differential Equations (with HomCont), User's Guide. Concordia University, Montreal, Canada.

- DOEDEL, E. AND KERNÉVEZ, J. 1986. AUTO: Software for continuation problems in ordinary differential equations with applications. Applied Mathematics, California Institute of Technology, Pasadena, CA.
- FEIGIN, M. I. 1994. *Forced Oscillations in Systems with Discontinuous Nonlinearities*. Nauka, Moscow. In Russian.
- FILIPPOV, A. F. 1964. Differential equations with discontinuous right-hand side. In *American Mathematical Society Translations, Series 2*. AMS, Ann Arbor, 199–231.
- FILIPPOV, A. F. 1988. *Differential Equations with Discontinuous Right-Hand Sides*. Kluwer Academic, Dordrecht.
- KUZNETSOV, YU. A., RINALDI, S., AND GRAGNANI, A. 2003. One-parameter bifurcations in planar Filippov systems. *Int. J. Bifurcation and Chaos* 13, 2157–2188.
- TONDL, A. 1970. *Self-Excited Vibrations*. Monographs and Memoranda, No. 9, National Research Institute for Machine Design, Běchovice.
- YOSHITAKE, Y. AND SUEOKA, A. 2002. Forced self-excited vibration with dry friction. In *Applied Nonlinear Dynamics and Chaos of Mechanical Systems with Discontinuities*, M. Wiercigroch and B. de Kraker, Eds. World Scientific, Singapore, 237–259.

Received June 2003; revised April 2004; accepted October 2004